



## The catalytic activity of manganese oxide catalysts for the toluene oxidation process

Tran Thị Thu Hien<sup>2,3</sup>, Nguyen Van Chuc<sup>1,4</sup>, Ly Bích Thuy<sup>2</sup>, Ta Dinh Quang<sup>1</sup>, Nguyen Thanh Hung<sup>1</sup>, Khong Manh Hung<sup>5</sup>, Le Minh Thang<sup>1\*</sup>

<sup>1</sup>School of Chemical Engineering, Ha Noi University of Science and Technology, 01 Dai Co Viet, Ha Noi, Viet Nam

<sup>2</sup>School of Environmental Science and Technology, Ha Noi University of Science and Technology, 01 Dai Co Viet, Ha Noi, Viet Nam

<sup>3</sup>Faculty of Natural Sciences, Quy Nhon University, 170 An Duong Vuong, Quy Nhon City, Binh Dinh, Viet Nam

<sup>4</sup>Tech-Vina, JSC, Binh Dan, Tan Dan, Khoai Chau, Hung Yen, Vietnam

<sup>5</sup>Institute for Chemistry and Material/Academy of Military Science and Technology, 17 Hoang Sam, Nghia Do Ward, Cau Giay District, Hanoi, Vietnam

\*Email: [thang.leminh@hust.edu.vn](mailto:thang.leminh@hust.edu.vn)

### ARTICLE INFO

Received: 02/3/2023

Accepted: 20/5/2023

Published: 30/6/2023

Keywords:

Manganese oxide catalysts,  
toluene oxidation

### ABSTRACT

Manganese oxide catalysts were prepared by several preparation methods, such as hydrothermal, sol-gel method, and characterized by XRD, BET, H<sub>2</sub>-TPR, SEM-EDS, and FT-IR. The catalytic activities of catalysts were evaluated through the toluene reaction at the temperature range of 150 °C – 400 °C. Among the catalysts, the @ MnO<sub>2</sub> 150 catalyst exhibited the highest catalytic activity. It could completely convert toluene into CO<sub>2</sub> at 300 °C. The larger specific surface area and lower reduction temperature enhance the higher activity of the @ MnO<sub>2</sub> 150 catalyst. Thus, the @ MnO<sub>2</sub> 150 catalyst is chosen to study in the subsequent research.

### Introduction

Volatile organic compounds (VOCs) are one of the environmental pollutants of concern because they contribute to polluted environmental phenomena such as photochemical smog and secondary particulate matter. Moreover, some VOC emitted from artificial activities seriously affects human health and the environment [1-10].

Following many previous studies, there are many methods to treat VOC. Catalytic oxidation is a common method to treat VOCs, such as toluene, benzene, and xylene [11]. Toluene is one of the aromatic VOCs that are used in industrial processes. It quickly evaporates under ordinary temperature and pressure conditions, increasing the exposure capacity and seriously affecting

human health. Thus, removing toluene from the exhaust gas mixture and protecting human health and the environment is an urgent duty.

For the VOC's complete oxidation, some noble metal-based catalysts such as Pd and Pt have been studied and demonstrated that possess high activity [12-15.] Besides, the noble metal-based catalyst has a limited supply, a high price, and is easily deactivated for aging conditions, so they are applied with difficulty in reality.

The transition metal-based catalyst is the alternative method for noble-metal because of its low price, high catalytic activity, and durability in some aging conditions, such as water vapor and sulfur compounds. Moreover, the oxygen vacancies in the oxidation reaction can be formed using the transition metal-based catalyst.

Manganese is one of the transition metals used in the oxidation reactions of CO and VOCs, at a cheap cost. Therefore, it has been studied and applied in industrial manufacturing. In some studies, Mn oxides can be divided into many forms, such as MnO, MnO<sub>2</sub>, Mn<sub>2</sub>O<sub>3</sub>, and Mn<sub>3</sub>O<sub>4</sub>. Their catalytic activity and application ability are affected primarily by the synthesis method [16].

On the contrary, the lattice oxygens can be formed in the structure of a manganese oxide catalyst instability. So, the oxygen can be stored in the crystal lattice, enhancing the catalytic activity in the CO and VOCs oxidation reactions. The oxidation states of manganese oxide also affect the catalytic activity. Therefore, there are many studies conducted to evaluate the effectiveness of removing VOCs process using the manganese base catalyst, such as n-hexane, benzene, and toluene [17-19].

From the evaluation of many studies, the oxidation states of Mn<sup>2+</sup>/Mn<sup>3+</sup> and Mn<sup>3+</sup>/Mn<sup>4+</sup> created a high activity, even, in some cases, the catalytic activity of the Mn oxide catalyst was higher than that of the Pt/TiO<sub>2</sub> catalyst in the oxidation reaction of ethyl acetate and n-hexane [20].

Thus, the manganese oxide catalyst can oxidize aromatic VOC species as toluene. The current research focuses on preparing the manganese oxide catalyst by many different methods and evaluating their activity in the toluene oxidation reaction.

## Experimental

### *Preparation of the catalysts*

For @ MnO<sub>2</sub> 120, @ MnO<sub>2</sub> 150 and β-MnO<sub>2</sub> catalyst, the method was successfully applied in studies of N. Huang et al [21] to synthesize single metal oxides of Mn, which is used in this study. The preparation process of catalyst by the hydrothermal method can be described following as:

For @ MnO<sub>2</sub>, 3.16 g KMnO<sub>4</sub> and 4.54 g H<sub>2</sub>C<sub>2</sub>O<sub>4</sub>·2H<sub>2</sub>O were diluted separately with 35 mL distilled water to form two solutions, and they were stirred to form homogeneous solutions. Then H<sub>2</sub>C<sub>2</sub>O<sub>4</sub>·2H<sub>2</sub>O solution was added drop wisely to the KMnO<sub>4</sub> solution under stirring for 30 min at 60 °C, then moved into a teflon lined stainless steel autoclave (200 mL), and the autoclave was heated to 120 °C for 12 hrs. The product was collected, washed, filtered, and dried at 80 °C for 12 hours. Finally, the collected solids were calcined at 400 °C for 5 hrs, then labeled and stored. The above

steps were repeated, and the solution in the autoclave was heated to 150 °C; the obtained catalysts were denoted as @ the MnO<sub>2</sub> 120 and @ the MnO<sub>2</sub> 150 catalysts, respectively.

For β-MnO<sub>2</sub> catalyst, 1.69 g MnSO<sub>4</sub>·H<sub>2</sub>O and 2.28g (NH<sub>4</sub>)<sub>2</sub>S<sub>2</sub>O<sub>8</sub> were diluted with 80 mL distilled water, then stirred magnetically for about 30 min to form a homogeneous solution before it was moved into a Teflon lined stainless steel autoclave (200 mL). After that, the solution in the autoclave was heated to 160 °C for 12 hrs in an oven. The product was collected, washed, filtered, dried at 80 °C, and then calcined at 300 °C for 5 hrs.

The MnO<sub>2</sub> catalyst was prepared by the sol-gel method. 4.62 mL Mn(NO<sub>3</sub>)<sub>2</sub> solution 50% was diluted with 60 mL distilled water, then 4.16 g citric acid was diluted with 16.64 mL distilled water; then, two solutions were mixed to form a homogeneous solution. The solution was heated to 60 °C and evaporated at this temperature until a sticky gel was obtained. The product was dried at 120 °C for 12 hrs and calcined at 500 °C in the air for 3 hrs at the heating rate of 1 min/°C.

### *Catalyst characterization*

The Micromeritics Gemini VII 2390 instrument was used to determine the specific surface areas of the catalysts at the GeViCat center, Hanoi University of Science and Technology.

The X-ray diffraction (XRD) patterns were measured by the D8 Advance Bruker instrument at the Faculty of Chemistry, Hanoi University of Science, Vietnam.

The Micromeritics Autochem II 2920 device at the GeViCat center, Hanoi University of Science and Technology was used to record the H<sub>2</sub>-TPR profile.

The IR spectra were measured by the Nicolet IS50 FT-IR spectrometer at the GeViCat center, Hanoi University of Science and Technology. SEM, EDS were characterized by using the JCM - 7000 divide (Benchtop SEM), GeViCat center, Hanoi University of Science and Technology.

### *Catalytic oxidation experiment*

The fixed-bed quartz microreactor was used to evaluate the catalytic activity. The size of the microreactor is 0.64 cm in inner diameter and 60 cm in length. The weight of the catalyst with particle sizes of 250–300 μm is 0.1 g for each experiment. The evaluating activities were conducted in the temperature range of 150 to 400 °C,

using a reactant flow containing 5000 ppm toluene in O<sub>2</sub> (N<sub>2</sub> as balance gas) at a 9.5 mL/min N<sub>2</sub> flow rate. An online gas chromatograph (GC) with a thermal conductivity detector (TCD) was used to detect the inlet and outlet toluene. The total inlet flow rate for toluene oxidation was 25 mL/min.

### Analysis and calculation of the results

The following equation determined the toluene conversion:

$$\eta (\%) = \frac{C^i - C^o}{C^i} \times 100 \quad (1)$$

Where  $\eta$ : toluene conversion (%);

$C^i$ : toluene concentration in the inlet flow (ppm);

$C^o$ : toluene concentration in the outlet flow (ppm).

The conversion of toluene into CO<sub>2</sub> was evaluated as equation 2:

$$\gamma (\%) = \frac{C_{CO_2}^o}{7(C^i - C^o)} \times 100 \quad (2)$$

Where,  $\gamma$ : the percent of toluene can be converted into CO<sub>2</sub> (%);

$C_{CO_2}^o$ : CO<sub>2</sub> concentration in the outlet flow (ppm).

## Results and discussion

### Characterization of the catalyst

#### BET surface

BET surface areas of the @ MnO<sub>2</sub> 150 and the  $\beta$  - MnO<sub>2</sub> catalyst are showed in Table 1.

Table 1: BET surface areas of the catalysts

No	Catalysts	BET surface area (m <sup>2</sup> /g)
1	@ MnO <sub>2</sub> 150	83.20
2	$\beta$ - MnO <sub>2</sub>	12.91

Depending on the preparation method, the MnO<sub>2</sub> catalyst has a different activity. Compared to the surface area of the catalyst, the @ MnO<sub>2</sub> 150 catalyst possessed surface areas around 83.20 m<sup>2</sup>/g, which was many times higher than that of the  $\beta$  - MnO<sub>2</sub> catalyst (12.91 m<sup>2</sup>/g). Moreover, following our previous studies, the surface area of the MnO<sub>2</sub> catalyst is 14.4 m<sup>2</sup>/g [22]. From this information can predict that the catalytic activity of the @ MnO<sub>2</sub> 150 catalyst may be

higher than that of the  $\beta$  - MnO<sub>2</sub> catalyst, MnO<sub>2</sub> catalyst.

#### TPR- H<sub>2</sub>

TPR-H<sub>2</sub> profiles of manganese oxides were used to give many explanations. Following some previous studies, the reduction process of MnO<sub>2</sub> can occur in stages: MnO<sub>2</sub> → Mn<sub>2</sub>O<sub>3</sub> → Mn<sub>3</sub>O<sub>4</sub> → MnO [23-24]. The reduction temperatures for each stage are different. The stage MnO<sub>2</sub> → Mn<sub>2</sub>O<sub>3</sub> can happen at low temperatures (about < 250 °C); the stage Mn<sub>2</sub>O<sub>3</sub> → Mn<sub>3</sub>O<sub>4</sub> occurs at 250 °C – 270 °C, and the stage Mn<sub>3</sub>O<sub>4</sub> → MnO occurs at 280 °C – 300 °C [23,25]. However, the stage MnO → Mn will occur at temperatures above 750 °C, so MnO is the final product in TPR-H<sub>2</sub> analysis [26].

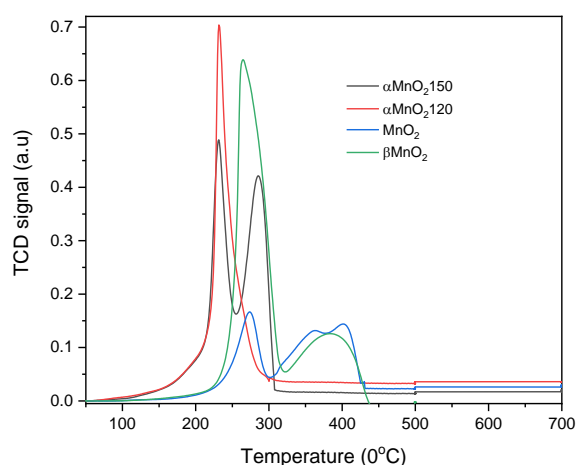


Figure 1: H<sub>2</sub> – TPR pattern of manganese oxide catalysts

Compare to the @ MnO<sub>2</sub> 150 catalyst, and the @ MnO<sub>2</sub> 120 catalyst, two catalysts were reduced at the same temperature (231 °C), but the @ MnO<sub>2</sub> 150 catalyst can be reduced at two temperatures (231 °C and 285 °C, respectively). Thus, the results showed that the @ MnO<sub>2</sub> 150 catalyst is reduced in 2 stages: MnO<sub>2</sub> → Mn<sub>2</sub>O<sub>3</sub>, then Mn<sub>2</sub>O<sub>3</sub> → MnO (Fig 1).

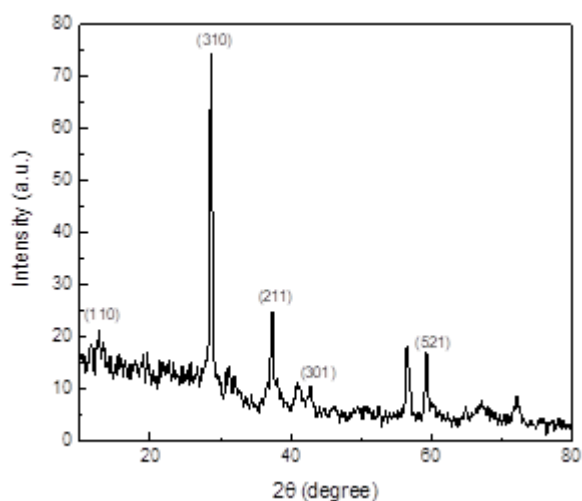
For the  $\beta$  -MnO<sub>2</sub> catalyst, It can be reduced in 2 stages: the stage Mn<sub>2</sub>O<sub>3</sub> → Mn<sub>3</sub>O<sub>4</sub>, and the stage Mn<sub>3</sub>O<sub>4</sub> → MnO. And MnO<sub>2</sub> catalyst, based on the XRD result [22], can be reduced in 2 stage Mn<sub>2</sub>O<sub>3</sub> → Mn<sub>3</sub>O<sub>4</sub>, Mn<sub>3</sub>O<sub>4</sub> → MnO.

Moreover, The @ MnO<sub>2</sub> 150,  $\beta$  -MnO<sub>2</sub> catalyst possesses a high H<sub>2</sub> quantity consumption (Table 2); therefore, they can exhibit excellent oxygen mobility, which explains why they have high activity at a lower temperature.

Table 2: Total H<sub>2</sub> consumption of manganese oxide Catalysts [22]

Catalysts	Temperature at maximum (°C)	Consumed hydrogen (mmol/g)	Total H <sub>2</sub> consumption (mmol/g)
@ MnO <sub>2</sub> 120	231	7.34	7.34
@ MnO <sub>2</sub> 150	231.3	5.06	9.43
	285.4	4.37	
β - MnO <sub>2</sub>	264.7	12.67	17.38
	382.5	4.71	
MnO <sub>2</sub>	272.4	0.77	2.33
	360.4	1.59	

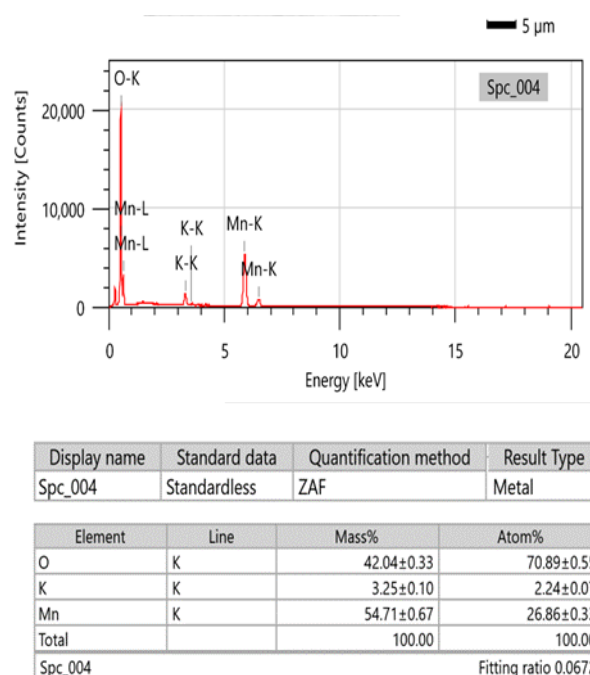
## XRD

Figure 2: XRD Pattern of the @ MnO<sub>2</sub> 150 catalyst

The XRD technique determined the crystal structure of the @ MnO<sub>2</sub> 150 catalyst. Figure 2 showed the diffraction peaks at 2θ: 12.6°; 18.2°; 28.6°; 37.3°; 42.8°; 59.3° respectively, which corresponds to the lattice (110), (200), (310), (211), (301), (521) [27]. The diffraction peaks indicate that the crystal phase of @ - MnO<sub>2</sub> belongs to the tetragonal crystal system with JCPDS Card No: 44-0141. Moreover, the crystalline sizes of the catalyst were determined by the Scherer equation [28] with 12.3 nm.

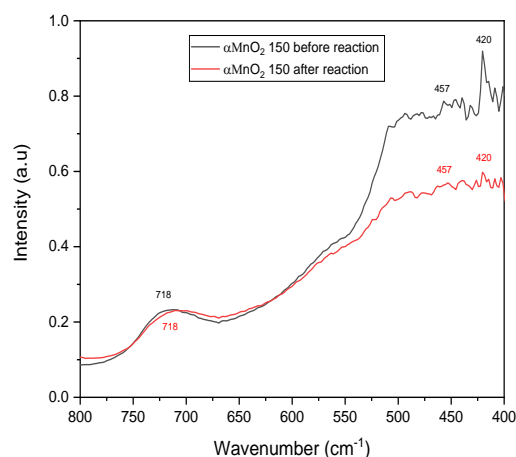
## EDS of catalyst

The elemental composition of the catalyst is shown in the following figure:

Figure 3: EDX profile and the element composition of the @ MnO<sub>2</sub> 150 catalyst

The results show the presence of K in the composition of the catalyst. From some previous studies, K<sup>+</sup> is an exchange cation in the α-MnO<sub>2</sub> structure to compensate for the negative charge generated when the cations Mn<sup>2+</sup> and Mn<sup>3+</sup> replace Mn<sup>4+</sup> in the MnO<sub>2</sub> structure [29].

## IR spectra of catalyst

Figure 4: The FTIR profile of the @ MnO<sub>2</sub> 150 catalyst before and after the reaction

The FTIR spectra of the catalyst from 800 to 400 cm<sup>-1</sup> are shown in Figure 4. The absorption bands in the region

<https://doi.org/10.51316/jca.2023.039>

are easily observed and characterized for Mn–O lattice vibration [30]. Some absorption bands at 420, 457, and 718  $\text{cm}^{-1}$  are the characteristic peaks of manganese oxides [30]. This result corresponds with the IR profile of  $\alpha\text{-MnO}_2$  in the study of Kang et al. [30]. Thus, water or chemical substances are not absorbed on the surface of the catalyst.

### Catalytic activity for toluene oxidation

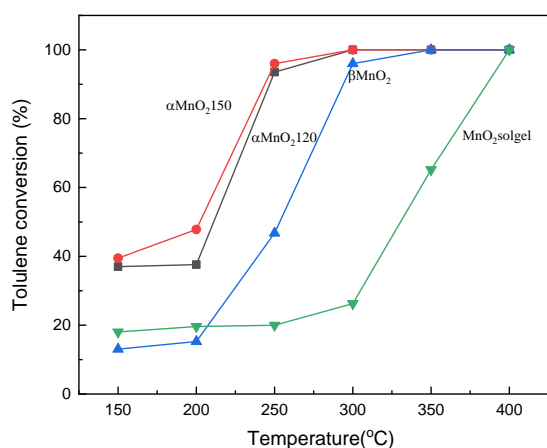


Figure 5: The result of evaluating catalytic activity

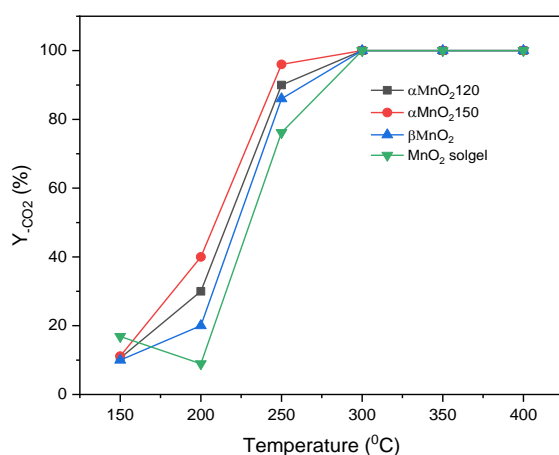


Figure 6: The percent of toluene that can be converted into  $\text{CO}_2$

The catalytic activity evaluating results are described in Figure 5, and Figure 6. The experiment was conducted with an inlet toluene concentration of 5000 ppm and a flow rate of 25 mL/min. As a result, a change in toluene conversion corresponds to the reaction time. The catalytic activities of the manganese oxide catalysts were shown in figure 1.4 at temperature ranges from 150 °C to 400 °C. At 150 °C, the toluene conversion of manganese oxide catalysts is still low, but as the temperature increases to 350 °C; the catalysts achieve a complete conversion, except for the  $\text{MnO}_2$  sol-gel catalyst. Experiment data also indicated that @  $\text{MnO}_2$

150 catalyst possesses the highest toluene conversion at 300 °C.

The yield of  $\text{CO}_2$  was shown in Fig 6. The percent of toluene is entirely converted into  $\text{CO}_2$  at 300 °C. In comparison, the yield of  $\text{CO}_2$  over manganese oxide catalysts was lower in regional temperature (150 °C – 250 °C), and the @  $\text{MnO}_2$  150 catalyst exhibited the highest yield of  $\text{CO}_2$ . Thus, the result clarified the influence of the preparation method on the @  $\text{MnO}_2$  150 catalyst's catalytic activity.

In the Huang studies [21], the  $\alpha@ \beta\text{-MnO}_2$  catalyst was synthesized by the hydrothermal method. The inlet toluene concentration is about 500 ppm, and the reaction results showed that toluene could completely convert at 205 °C. In the study, the @  $\text{MnO}_2$  150 catalyst (5000 ppm toluene,  $T_{100} = 300$  °C.) has an inlet toluene concentration higher than ten times. Therefore, it is difficult to determine that the @  $\text{MnO}_2$  150 catalyst is not as good as the  $\alpha\beta\text{-MnO}_2$  catalyst. Moreover, the @  $\text{MnO}_2$  150 catalyst was synthesized more simply than the  $\alpha\beta\text{-MnO}_2$  catalyst. Thus, the @  $\text{MnO}_2$  150 catalyst can be applied in removing the exhaust gas containing toluene.

### Conclusions

In conclusion, the manganese oxide catalysts were synthesized by many different preparation methods, such as hydrothermal and sol-gel. The  $\alpha\text{-MnO}_2$  150 catalyst exhibited the highest catalytic activity in the toluene oxidation process. Some modern techniques as BET, TPR-  $\text{H}_2$ , FT – IR and EDS were used to demonstrate the reason caused the high activity. As can be seen, the  $\alpha\text{-MnO}_2$  150 catalyst has the crystal phase of  $\alpha\text{-MnO}_2$  and belongs to the tetragonal crystal system with JCPDS Card No: 44-0141. Moreover, the catalyst also possessed higher surface areas, low reduction temperature, and the highest  $\text{H}_2$  quantity consumption, which explains that it has high activity at a low temperature. Therefore, the hydrothermal method was chosen to prepare the manganese oxide catalyst. .

### Acknowledgments

The authors thank the Ministry of Science and Technology of Vietnam for sponsoring the experimental work under project number ĐTĐL.CN-68/19. Thi Thu Hien Tran thanks the RoHan Project funded by the German Academic Exchange Service (DAAD, No. 57315854) and the Federal Ministry for Economic Cooperation and Development (BMZ) inside the

<https://doi.org/10.51316/jca.2023.039>

framework "SDG Bilateral Graduate school programme for a PhD scholarship and JSC Vingroup, VINIF, Institute of Big Data for the Master, PhD Scholarship Programme of Vingroup Innovation Foundation (VINIF).

## References

1. W. G. Tucker, Digital Engineering Library @McGraw-Hill, 2001.
2. R. M. Heck, R. J. Farrauto, Wiley-Interscience, 2009.
3. A. C. Lewis, N. Carslaw, P. J. Marriott, R. M. Kinghorn, P. Morrison, A. L. Lee, K. D. Bartle, M. J. Pilling, *Nature* 405 (2000) 778–781. <https://doi.org/10.1038/35015540>
4. I. C. Marcu, A. Urda, I. Popescu, V. Hulea, *IGI Global* (2017) 59–121. <https://doi.org/10.4018/978-1-5225-0492-4.ch003>
5. M. J. Molina, F. S. Rowland, *Nature* 249 (1974) 810–812. <https://doi.org/10.1038/249810a0>
6. M. Amann, M. Lutz, *J. Hazard. Mater.* 78( 2000) 41–62. [https://doi.org/10.1016/s0304-3894\(00\)00216-8](https://doi.org/10.1016/s0304-3894(00)00216-8)
7. S. Ascaso, M. E. Gálvez, P. Da Costa, R. Moliner, M. Jesús Lázaro Elorri, *Comptes Rendus Chimie* 18 (2015) 1007–1012. <https://doi.org/10.1016/j.crci.2015.03.017>
8. L. Lazar, H. Koeser, I. Fechet, I. A. Balasanian *Revista de Chimie* 71 (2020) 79–87. <https://doi.org/10.37358/Rev. Chim.1949>
9. B. J. Finlayson-Pitts, J. N. Pitts Jr, *Science* 276 (1999) 1045–1051. <https://doi.org/10.1126/science.276.5315.1045>
10. M. Stoian, L. Lazar, F. Uny, I. Fechet, *Revista Chimie* 71 (2020) 97–113. <https://doi.org/10.37358/RC.20.7.8229>
11. M. Alifanti, M. Florea, V. I. Pârvulescu, *Applied Catalysis B: Environmental* 70 (2007) 400–405. <https://doi.org/10.1016/J.APCATB.2005.10.037>
12. A.K. Datye, J. Bravo, T.R. Nelson, P. Atanasova, M. Lyubovsky, L. Pfefferle, *App. Catal. A*, 2000, 198, 179–196.
13. Y.H. Chin, C. Buda, M. Neurock, E. Iglesia, *J. Am. Chem. Soc.* 135 (2013) 15425–15442. <https://doi.org/10.1021/ja405004m>
14. H. Xiong, K. Lester, T. Ressler, R. Schlögl, L.F. Allard, A.K. Datye, *Catal. Lett.* 147 (2017) 1095–1103. <https://doi.org/10.1007/s10562-017-2023-7>
15. X. Zou, Z. Rui, H. Ji, *ACS Catal.* 7 (2017) 1615–1625 <https://doi.org/10.1021/acscatal.6b03105>
16. M. S. Kamal, S. A. Razzak, M. M. Hossain, *Atmos. Environ.* 140 (2016) 1117–134. <https://doi.org/10.1016/j.atmosenv.2016.05.031>
17. C. Lahousse, A. Bernier, E. Gaigneaux, P. Ruiz P, P. Grange, B. Delmon, *Proceedings of the 3rd World Congress on Oxidation Catalysis* 1997 777–785. [https://doi.org/10.1016/S0167-2991\(97\)81040-3](https://doi.org/10.1016/S0167-2991(97)81040-3).
18. J. Luo., Q. Zhang, A. Huang, S. L. Suib, *Micropor. Mesopor. Mat.* 35–36 (2000) 209–217. [https://doi.org/10.1016/S1387-1811\(99\)00221-8](https://doi.org/10.1016/S1387-1811(99)00221-8)
19. F. N. Agüero, A. Scian, B. P. Barbero, L. E. Cadús, *Catal. Today* 133 – 135 (2008) 493–501. <https://doi.org/10.1016/j.cattod.2007.11.044>
20. Q. Sun, L. Li, H. Yan, X. Hong, K.S. Hui, Z. Pan, *J. Chem. Eng.* 242 (2014) 348–356. <https://doi.org/10.1016/j.cej.2013.12.097>
21. N. Huang, Z. Qu, C. Dong, Y. Qin, X. Duan, *Appl Catal A* 560 (2018) 195–205. <https://doi.org/10.1016/j.apcata.2018.05.00>
22. T. T. H. Tran, B. T. Ly, T. M. P. Pham, M. T. Le, *Vietnam Journal of Catalysis and Adsorption*, 10 (2021). <https://doi.org/10.51316/jca.2021.068>
23. Li J., Li L., Wu F., Zhang L., Liu X, *Catal. Comm.* 31 (2017) 52–56. <https://doi.org/10.1016/j.catcom.2012.11.013>
24. V. P. Santos M. F. R. Pereira, J. J. M. Orfao, J. I. Figueiredo, *Appl. Catal.B: Environ.* 99 (2010) 353–363. <https://doi.org/10.1016/j.apcatb.2010.07.007>
25. W. Tang, X. Wu, D. Li, G. Liu, H. Liu, Y. Chen, *J. Mater. Chem. A* 2 (2014) 2544–2554. <https://doi.org/10.1039/C3TA13847J>
26. Q. Ye, J. Zhao, F. Huo, J. Wang, S. Cheng, T. Kang, H. Dai, *Catal.Today* 175 (2011) 603–609. <https://doi.org/10.1016/j.cattod.2011.04.008>
27. V. Sannasi, K. Subbian, *J. Mater. Sci.: Mater. Electron.* 31 (2020) 17120–17132. <https://doi.org/10.1007/s10854-020-04272-z>
28. W. Yang, Y. Peng, Y. Wang, H. Liu, Z. Su, W. Yang, J. Chen, W. Si, J. Li, *Applied Catalysis B: Environmental*, 278 (2020). <http://doi.org/10.1016/j.apcatb.2020.119279>
29. X. Wang, Y. Li, *Chem. Eur. J.* 9 (2003) 300–306. <https://doi.org/10.1002/chem.200390024>
30. L. Kang, M. Zhang, Z. H. Liu, K. Ooi, *Spectrochim. Acta A Mol. Biomol. Spectrosc.* 67 (2007) 864–869. <https://doi.org/10.1016/j.saa.2006.09.001>